Correlation Between Pairing Initiation Sites, Recombination Nodules and Meiotic Recombination in *Sordaria macrospora*

Denise Zickler, Patrick J. F. Moreau, Anh Dao Huynh and Anne-Marie Slezec

Institut de Génétique et Microbiologie, Université Paris-Sud, Centre d'Orsay, 91405 Orsay-Cedex, France

Manuscript received October 10, 1991
Accepted for publication May 12, 1992

ABSTRACT

The decrease of meiotic exchanges (crossing over and conversion) in two mutants of *Sordaria macrospora* correlated strongly with a reduction of chiasmata and of both types of "recombination nodules." Serial section reconstruction electron microscopy was used to compare the synapsis pattern of meiotic prophase I in wild type and mutants. First, synapsis occurred but the number of synaptonemal complex initiation sites was reduced in both mutants. Second, this reduction was accompanied by, or resulted in, modifications of the pattern of synapsis. Genetic and synaptonemal complex maps were compared in three regions along one chromosome arm divided into well marked intervals. Reciprocal exchange frequencies and number of recombination nodules correlated in wild type in the three analyzed intervals, but disparity was found between the location of recombination nodules and exchanges in the mutants. Despite the twofold exchange decrease, sections of the genome such as the short arm of chromosome 2 and telomere regions were sheltered from nodule decrease and from pairing modifications. This indicated a certain amount of diversity in the control of these features and suggested that exchange frequency was dependent not only on the amount of effective pairing but also on the localization of the pairing sites, as revealed by the synaptonemal complex progression in the mutants.

THE mechanism by which two homologous chromosomes pair remains one of the least understood step of meiosis. The correlated effect of several mutations on both recombination and synapsis suggests a dependence of one upon the other (reviewed in BAKER *et al.* 1976; GIROUX 1988; ROEDER 1990) and precise timing with synchronous cultures of yeast confirmed that pairing and recombination are temporally related (PADMORE, CAO and KLECKNER 1991). Several recent observations suggest that at least the early stages of recombination may be required for pairing (ALANI, PADMORE and KLECKNER 1990; ENGEBRECHT, HIRSCH and ROEDER 1990; CAO, ALANI and KLECKNER 1990; BHARGAVA, ENGEBRECHT and ROEDER 1992).

When synapsed, each pair of homologs is connected by the meiosis-specific structure called synaptonemal complex (SC). This structure may also be implicated in recombination and chiasma formation. In some organisms segments of SC are retained at the chiasma sites (VON WETTSTEIN, RASMUSSEN and HOLM 1984). Frequencies of the SC-associated nodules correlate well with the chiasma frequencies in several species and both show similar nonrandom distribution along the bivalents (reviewed in VON WETTSTEIN, RASMUSSEN and HOLM 1984; CARPENTER 1988). Nevertheless, one important question remains open: does SC initially assemble at random sites, and if not, how do these sites relate to the amount and/or distribution of chiasmata? In most organisms, the pattern of distribution of chiasmata along chromosomes is not random (JONES 1984, 1987; CARPENTER 1988; KING and MORTIMER 1990). Incomplete or localized pairing has often been advanced to explain chiasma localization. The analysis of several species has shown that, indeed, in some cases, localized chiasmata are related to localized pairing (FLETCHER 1977; OAKLEY and JONES 1982; MOENS and SHORT 1983; STACK and SOULLIERE 1984; BERNELOT-MOENS and MOENS 1986; LOIDL 1987; CROFT and JONES 1989). Sex chromosomes are other examples of correlated localized pairing and recombination (HOLM and RASMUSSEN 1983; SOLARI, FECHHEIMER and BITGOOD 1988; SPYROPOULOS, WISE and MOENS 1989; SUDMAN and GREENBAUM 1990). However, these examples do not account for the vast majority of organisms which exhibit very different patterns of chiasma distribution, although they show full synapsis (reviewed in JONES 1984, 1987; VON WETTSTEIN, RASMUSSEN and HOLM 1984).

Increased or decreased chiasma frequencies as a result of changes of pairing sites is suggested in studies of chromosome rearrangements (MAGUIRE 1986; PARKER 1987) and in the presence of B chromosomes (THOMSON, WESTERMAN and MURRAY 1984; PARKER *et al.* 1990). Such changes could also be invoked to account for the chiasma frequencies affected by environmental or experimental factors, where reduced chiasmata are found to correlate with lowered synapsis

and SC assembly (HENDERSON 1988; LOIDL 1989).

Therefore, to understand better the role of SC in mediating and/or regulating recombination events, a search for mutants which reduce recombination but do not cause SC arrest or major abnormalities was done in the Ascomycete *Sordaria macrospora*. In particular, the aim of this study was to provide insights into the important question of how the central component assembly sites of the SC correlate with the distribution of reciprocal exchanges among and along the bivalents. Our knowledge about distribution of SC initiation sites is based largely on observations of species with long chromosomes where interstitial sites are frequent, since pairing is mainly initiated from the telomeres in species with shorter chromosomes (VON WETTSTEIN, RASMUSSEN and HOLM 1984; RASMUSSEN 1986). In higher plants the number of pairing initiations widely exceed the number of chiasmata (HOLM 1977; ABIRACHED-DARMENCY, ZICKLER and CAUDERON 1983; HASENKAMPF 1984; GILLIES 1985; STACK and ANDERSON 1986a) and no correlation between the sequence of pairing and the chiasma localization was seen in two Allium species with similar patterns of pairing but different patterns of chiasmata distribution (ALBINI and JONES 1987, 1988).

The two mutants examined in this study show an overall 40% reduction in recombination, but the mutations have no obvious effect on the morphology of the SC. The effects of both mutations were defined over the whole genome, but also in detail along one chromosome arm. For this purpose, this arm was divided in four regions defined by translocation breakpoints, allowing comparison between the physical and genetical maps (ZICKLER *et al.* 1984; LEBLON, ZICKLER and LEBILCOT 1986). Sordaria shows few SC interstitial initiations (ZICKLER 1977), thus avoiding the problem of an excess of sites compared with the amount of chiasmata. The dissection of zygotene is possible with the use of serial sections, and variations in the course of synapsis in the two mutants were compared to the wild-type pattern. Additional investigation of the relationship between the processes of pairing and of recombination has been obtained by examining the location of the two types of SC nodules (CARPENTER 1979a, 1987) along the bivalents at different stages of zygotene and pachytene. The present study suggests a correlation between pairing-initiation sites, recombination nodules, chiasmata and recombination.

MATERIALS AND METHODS

Organism: *Sordaria macrospora* is an homothallic Ascomycete in which a single haploid nucleus carries all the information necessary to produce the whole cycle from spore to spore. All mutant strains used in the present study were derived from a wild-type stock, St Ismier, FGSC 4818. The media were previously described in ZICKLER *et al.* 1984.

Strains and genetic markers: Wild-type *S. macrospora* strains sporulate with 100% efficiency. The screen developed to identify mutants defective in meiotic disjunction was based on the assumption that their meiotic products would be aneuploid and, therefore, the spores abnormal or inviable. The recessive *spo76* mutant was isolated from protoplasts mutagenized by EMS (1% in isotonic buffer for 2 hr). After regeneration, the mycelia shooting aborted spores were easily detected, and *spo76* was scored as a colony producing almost no ascospores (<1 per 20 perithecia which corresponds to almost 1 per 4000 meioses). The *spo76-1* mutant showed wild-type growth and was highly UV and X-ray sensitive (HUYNH, LEBLON and ZICKLER 1986). This mutant formed axial elements during leptotene. Zygotene and pachytene nuclei (15 reconstructed) showed only short SC stretches (with a range of 2–7 nodules). When engaged in a piece of SC, the lateral elements were normal but between the SCs, the unsynapsed axial elements were split and appeared as two thin threads widely separated (over 500 nm) and sometimes broken. When observed using light microscopy, the diplotene and metaphase nuclei showed 28 chromosomes instead of the 7 wild-type bivalents or the 14 univalents seen in the 10 asynaptic mutants studied in *S. macrospora*. Almost all asci (99%) abort at or after anaphase I. The *SPO76* gene product was suggested to be required for cohesiveness of sister-chromatids during meiosis, as deduced from the phenotype of the mutant which showed split SC axial elements and early centromere division (MOREAU, ZICKLER and LEBLON 1985).

As a homozygote, the *asy2-17* mutant sporulates well: 95% of the asci form 8 viable ascospores. This mutant was one of the 34 mutants isolated as suppressor of *spo76-1*. Ultraviolet mutagenesis performed on *spo76* mycelia allowed the recovery of 37 revertants (screened for their ability to restore totally or partially the sporulation defect of *spo76*). The cross of each revertant to wild type led to the reappearance in the progeny of the original *spo76* mutation in 34 out of the 37 backcrosses. The 34 suppressors were then isolated from the nonparental ditype or tetratype asci. All suppressors were recessive (no dead spores in their crosses to wild type), and a complementation study allowed their assignment to six different genes (designated *ASY1* to *ASY6*) mapped on 5 of the 7 chromosomes of *S. macrospora*. All rescued the early equational separation of sister centromeres and the meiotic arrest of *spo76*, suggesting that they act at an earlier step in meiotic prophase I (HUYNH, LEBLON and ZICKLER 1986).

Most genetic markers used in this study were described previously (ZICKLER *et al.* 1984; LEBLON, ZICKLER and LEBILCOT 1986). The wild-type strain was isolated from one spore and all mutageneses were performed on this strain. Each mutant, (isolated from this strain) was backcrossed at least five times to wild type and all mutations segregated in a 2 to 2 ratio. The frequencies of the three tetrad types–parental ditype (PD), tetratype (T) and nonparental ditype (NPD)–were used to obtain estimates of the distances as follows: map units = T + 6 NPD/2 × total tetrads (PERKINS 1962). Calculation of exchange frequencies was deduced from the distribution of the three types of tetrads: zero exchange = PD − NPD, one exchange = T − 2 NPD and two exchanges = 4 × NPD except when NPD > PD; in this case one exchange = T − (PD + NPD) and two exchanges = 2 × (PD + NPD). Gene orders were based on the analysis of three-point crosses. The effects of *spo76* and *asy2-17* on exchange events were studied in three intervals on chromosome 2 and by modification of second division segregation frequencies of at least one marker per chromosome.

Cytology: For electron microscopy preparations, asci were fixed in 2% glutaraldehyde in phosphate buffer (pH

7) for 3 hr, post-fixed in 2% phosphate buffered osmium tetroxide for 1 hr and dehydrated through an alcohol series. Single asci were embedded in Epon 812 at 60° for 24 hr. Serial sections were stained with 5% aqueous uranyl acetate for 30 min followed by lead citrate for 10 min. Pictures were taken at a magnification of 8000. Three-dimensional reconstructions were performed as follows. The SC elements and nuclear structures from five consecutive sections were traced onto acetate sheets and when the nucleus was completed, each bivalent was redrawn on a new sheet with its relevant section numbers, centromere, synapsis regions, and nodule sites. The projected lengths were measured and the chromosome lengths were calculated using the Pythagorean theorem (with a mean section thickness of 80 nm). One hundred and ten wild-type nuclei were reconstructed: they cover leptotene, zygotene, pachytene and diplotene. For each mutant strain, four leptotene, 35 (+/*spo76*) and 36 (*asy2-17/asy2-17*) zygotene nuclei and three pachytene nuclei were analyzed. SC lengths and nodule positions were calculated on a Sharp microcomputer and the chromosome comparisons were made on a HP 1000 computer.

RESULTS

The two mutant strains show reduced recombination rates: Mutant *spo76-1* was highly defective in sporulation as a homozygote but the heterozygous strain sporulated to the same extent as wild type. The levels of sporulation seen in strains homozygous for *asy2-17* were close to those observed in the control, and only 5% of the asci showed inviable ascospores due to abnormal disjunction at meiosis I and subsequent production of aneuploid meiotic products.

The segregation of centromere-linked markers demonstrated that all the asci arose by a normal reductional division followed by normal second division segregation (SDS). SDS frequencies were estimated in one to three intervals for each of the seven chromosomes in the three strains (Table 1). Compared to wild type, a decrease of SDS frequencies was observed for all loci genetically linked to their centromere, in +/*76* (mean of 65%, with a range of 41 to 84% of the wild-type values) and in *asy2-17/asy2-17* (32–71%, mean of 54%). Among the five distal markers tested, which consequently had a SDS close to or higher than 66%, two in +/*76* and four in *asy2-17/asy2-17* showed also a decrease (range: 53–71%).

Conversion rates were calculated in the spore-color *PAM2* gene (Table 2). Conversion events occurred equally to wild type (6 wt:2 mutant asci) and to mutant (2 wt:6 m). No postmeiotic segregations were found in the analyzed asci. Mutation *asy2-17* reduced conversion more severely (31% of control) than +/*76* (71%). A reduction was also found when *asy2-17* was heterozygous (53% of control) and when associated with +/*76* either homozygous (41%) or heterozygous (33%). Unfortunately the conversion rates of the other seven known spore-color genes of *S. macrospora* are too low (<0.01%) to allow a comparison between mutants and wild type.

The number of chiasmata and recombination nodules was reduced in the two mutant strains: Wild-type strains have a minimum of two chiasmata per bivalent and the mean total number of chiasmata observed in 50 diplotene nuclei was 21 ± 3 over the seven bivalents. Heterozygous *spo76* and homozygous *asy2-17* strains (20 nuclei in diplotene were examined in using light microscopy for each) showed, respectively, 13–16 and 10–13 chiasmata per meiosis. Thus, despite recombination and chiasma defects, these two strains exhibited nearly wild-type levels of chromosome disjunction and subsequent viable haploid progeny. In contrast, double-mutants *asy2-17/asy2-17; +/76* with lower chiasma rates (range 8–11) and *asy2-17/asy2-17; 76/76* with rates below the minimum number of one per bivalent (range 2–6), showed more univalents and consequently increased aneuploidy (respectively 10% asci with unviable spores and 40 viable spores per perithecium instead of 800–1000), but progress through meiosis was unimpaired.

The extent of SC formation was used to define the temporal sequence of the zygotene nuclei in parallel with ascus growth and morphological changes undergone by the nucleolus. Homogeneously dense at leptotene, with a central "hole" which increases in size from mid-zygotene to pachytene (almost a ring at late pachytene), the nucleolus shows several small "holes" at diplotene.

Two morphological types of nodules were observed in the three strains. They were only found associated with synapsed elements. The ovoid large nodules (abbreviated "LN"), 60–80 nm wide in cross sections and 60 × 150 nm long in longitudinal sections, were of high electron density. Located on the central element, with their long axes parallel to the SC axis, they were always positioned in the central region of the SC (Figure 1). The small nodules ("SN") were more spherical, 40–60 nm wide and their density was always less than that of the large nodules (Figure 2). In contrast to the LN, their shape was less regular. They appear as soon as pairing is initiated and were frequently seen at the pairing forks (Figure 2).

In wild-type nuclei the number of LN increased from early to late zygotene. The same increase during zygotene was observed in the two mutant strains but the average number of nodules was reduced to about 70% (+/*76*) and 55% (*asy2-17/asy2-17*) of the wild-type values (Figure 3). The mean number of LN per late zygotene nuclei was 25.5 in the wild-type strain (range 24–26), 18 in +/*76* (range 17–20) and 14 (range 12–17) in *asy2-17/asy2-17*. In wild type, the number of LN decreased from late zygotene to mid-pachytene (mean of 23 with a range of 20–24 in 15 nuclei) and remained stable from mid-pachytene to diplotene (range of 19–23 in 10 diplotene nuclei). In wild type, pachytene must be shorter than the zygotene stage because fewer pachytene than zygotene

TABLE 1

Percentage of second division segregation for 13 genetic markers in wild type and mutant strains

Marker	Chromosome	Wild type	SDS/total	+/76	SDS/total	asy2-17/ asy2-17	SDS/total
yas2	1 right	66.0 ± 1.8	427/644	65.8 ± 1.6	561/853	34.8 ± 1.5	353/1013
yas3	1 left	54.2 ± 2	321/592	30.1 ± 1.6	247/819	24.0 ± 1.3	230/958
asy1-77	2 left	31.6 ± 4.8	31/98	13.0 ± 3.3	13/100	NT	NT
wam1	2 left	48.0 ± 2	289/602	22.7 ± 0.9	499/2201	NT	NT
lys2	2 left	56.9 ± 3.4	119/209	39.2 ± 4.4	47/120	28.6 ± 3.5	46/161
gsn1	3 left	74.3 ± 1.6	545/733	50.9 ± 1.8	373/733	50.5 ± 1.5	527/1043
pam2	4 right	61.8 ± 0.4	7143/11,547	52.2 ± 0.5	5420/10,380	44.0 ± 1.3	614/1394
yas1	4 left	49.9 ± 1.6	499/999	36.2 ± 1.2	544/1504	18.7 ± 0.7	487/2605
gas1	5 right	64.9 ± 1.6	581/895	62.2 ± 1.7	467/751	63.5 ± 2.7	193/304
gsn2	5 right	65.7 ± 2.1	338/514	71.3 ± 1.5	652/915	39.4 ± 1.8	293/744
thr1-18	5 left	31.5 ± 3.4	57/181	20.3 ± 2.8	40/197	20.7 ± 3.2	33/159
leu3-6	6 left	56.8 ± 3.8	96/169	40.2 ± 3.9	64/159	18.5 ± 3.1	28/151
sgr4	7 left	25.0 ± 3.4	41/164	19.0 ± 3.2	28/147	14.7 ± 2	44/300

Percentage = $p \pm \sqrt{\frac{p \times (100 - p)}{N}}$ where N = total number of asci. NT = not tested; SDS = second division segregation.

TABLE 2

***PAM2* conversion rates in wild type and mutant strains**

Strains	SDS Rates (No. SDS/total)	Conversion rates
Wild type (+)	61.8 ± 0.4 (7143/11,547)	232/17,704 = 1.31%
+/spo76	52.2 ± 0.5 (5420/10,380)	263/28,017 = 0.93%
asy2-17/asy2-17	44.0 ± 1.3 (614/1394)	31/7585 = 0.40%
asy2-17/+	56.7 ± 1.2 (940/1658)	50/7182 = 0.70%
asy2-17/+; +/spo76	39.4 ± 1.2 (636/1615)	35/8069 = 0.43%
asy2-17/asy2-17; +/spo76	27.7 ± 1.7 (177/640)	34/6321 = 0.54%

232/17,704 = 232 conversion events among 17,704 asci. Percentage of second division segregation (SDS) for *PAM2* = $p \pm \sqrt{\frac{p \times (100 - p)}{N}}$ where N = total number of scored asci.

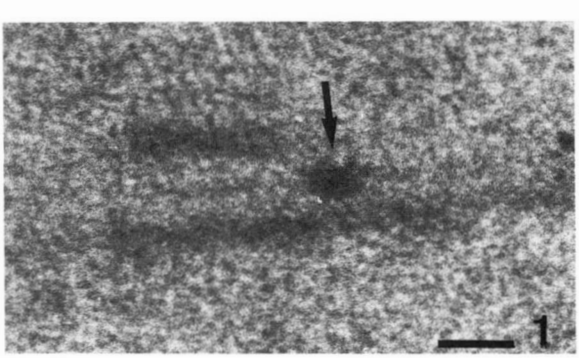

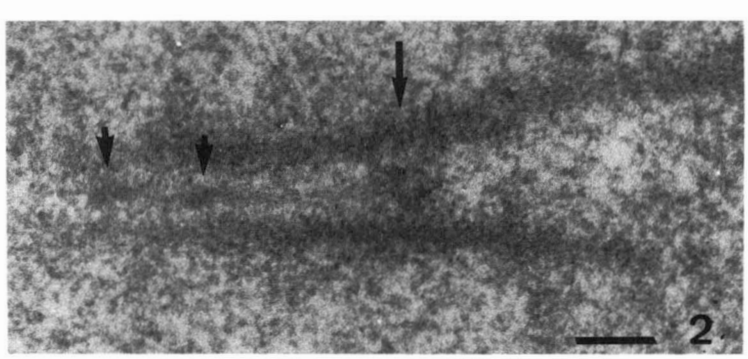

FIGURE 1.—Segment of pachytene SC (electron micrograph) showing a large nodule (arrow) intimately associated with the central element. Bar = 0.1 μm.

FIGURE 2.—Ultrastructure of two small nodules (small arrows) at early zygotene. Arrow points to the pairing fork of two homologous chromosomes. Bar = 0.1 μm.

nuclei were found. This is even accentuated in the mutant strains. If the wild-type establishment of the temporal relationship between these nuclei (based on nucleolus morphology and ascus growth) was applied here, although not completely paired, the three mutant nuclei with arrowheads in Figure 3 should be mid-pachytene nuclei. They contain 17, 18 and 17 LN in *+/76* and 14, 15 and 14 LN in *asy2-17/asy2-17*, which represents respectively 75 and 62% of the wild-type numbers. Thus, the effect of mutations on LN closely parallels their effects on recombination and chiasmata.

The mutations did not affect the distribution of LN among the bivalents. There is a difference in mean

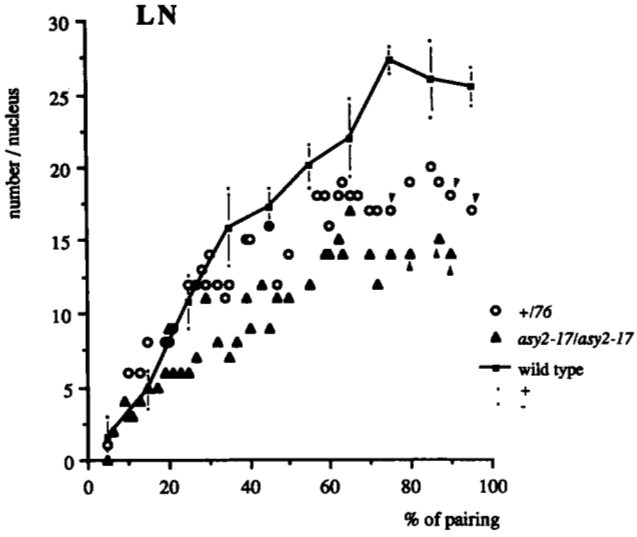

FIGURE 3.—Number of large nodules (LN) per nucleus. Wild type is represented as the mean (+ and − = standard deviation shown for each point). Mutants presented as individual nuclei. All mutant scores are under the standard deviation for wild type beyond 60% pairing. Mutant nuclei indicated with arrowheads are pachytene nuclei according to wild-type staging.

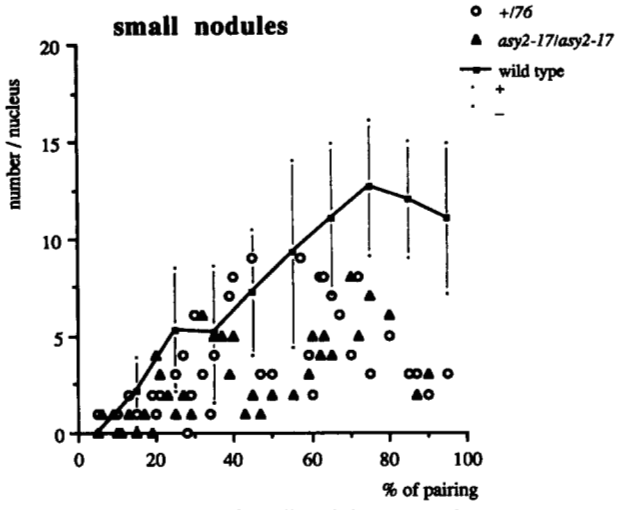

FIGURE 4.—Number of small nodules per nucleus *vs.* percentage of pairing in the nuclei. Presentation is the same as that shown in Figure 3.

LN per SC length between the longest and the shortest bivalents: 0.45 and 0.64 LN per μm of SC in wild type, 0.31–0.5 in *+/76* and 0.23–0.43 in *asy2-17/asy2-17* while the mean number of LN per SC length for the whole SC set was, respectively, of 0.56, 0.4 and 0.31. Thus the frequency of LN per μm length of SC was higher in small than in larger chromosomes but the differences were of the same order of magnitude in the three strains.

Figure 4 presents the number of SN at different substages of zygotene. Compared to the wild-type distribution, it was clear that the total number was lower in the two mutant strains, especially after mid-zygotene. In addition, the SN frequency decrease

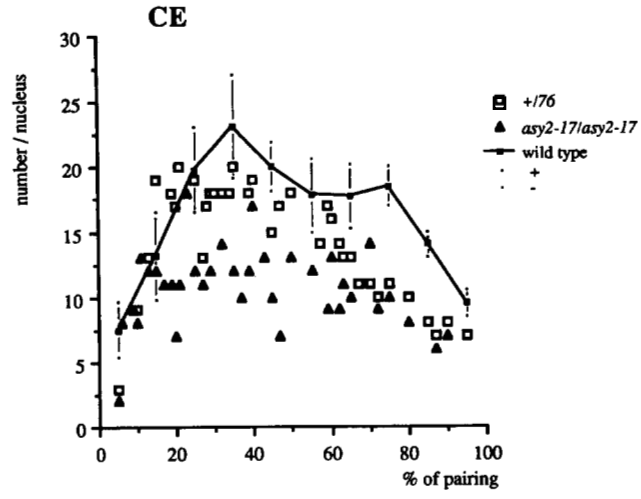

FIGURE 5.—Number of central elements (CEs) per nucleus *vs.* percentage of pairing in the nuclei. In wild type, + and − = standard deviation shown for each point. Presentation is the same as that shown in Figure 3.

paralleled that of the LN. In wild type, SN were no longer visible after mid-pachytene.

Since the lower total number of nodules in the two mutant strains appeared to be an early event in zygotene, we wondered if this defect was related to pairing. The SC initiation sites were therefore mapped in the three strains.

There was a clear parallel between the reduction of large and small nodules and the reduction of the number of sites of SC initiation in the two mutant strains: In *S. macrospora* axial elements were formed during leptotene and full-length axial elements were observed in all late leptotene nuclei. At the end of leptotene, and preceding central element (CE) formation, almost all homologs were found roughly aligned in the three strains.

Initial CE formation occurred most often in the bivalent regions near the telomeres. As seen in Figure 5, until pairing was 35% complete, the number of CE segments increased rapidly in the three strains. Above 35%, the mean length of CE increased and the number of segments decreased by fusion of adjacent sites as SC formation proceeded. In the wild-type strain, this decrease either stabilized, or new intercalary segments were formed in mid-late zygotene (from 60 to 75% total pairing). The two mutants showed a progressive drop of the number of CE as pairing approached completion (Figure 5). A second difference between wild type and mutants is evident from Figure 5: the number of SC initiation sites was and remained lower in the mutants, and this difference was most obvious for *asy2-17/asy2-17*.

No periodicity or uniformity in the distances between adjacent CE initiation sites was found, either in the wild type or in the two mutant strains. Parallel to the distribution of the nodules, the number of sites in wild-type mid-zygotene nuclei was higher in the long-

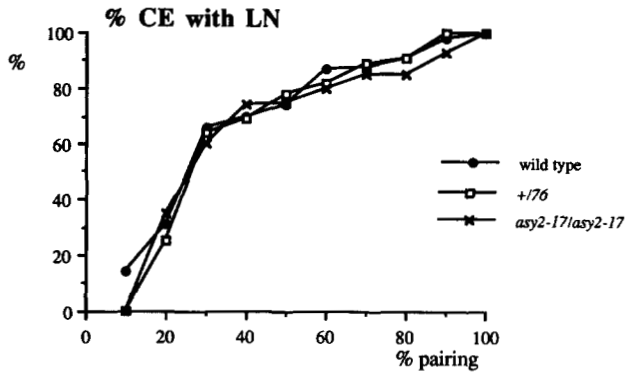

FIGURE 6.—Percentage of central elements (CE) with large nodules (LN) *vs.* percentage of pairing: there is no significant difference between wild type and mutants in the percentage of CE having large nodules among all observed CEs.

est bivalent 1 (range 2–7) compared to the shortest bivalent 7 (range 1–3). The same was true also for the mutants: respectively, 1–5 and 1–3 in +/*76* and 1–4 compared to 0–2 in *asy2-17/asy2-17*.

The SC segments observed during zygotene did not all contain nodules. Among the SC segments observed during zygotene, we determined if the percentage of segments with nodules was equal in both wild type and mutants. Figure 6 shows clearly that equivalent potential attachment sites for LN were utilized in the three strains. Therefore, although the number of CE was reduced in the two mutants, the number of LN per segment was not, indicating that the reduction in synaptic initiations would seem to be the primary defect.

The degree of synchrony of pairing between the 7 bivalents was different in the mutant strains: Completely unpaired homologs were found only in very early wild-type zygotene nuclei (below 20% paired). Although a clear difference in speed of synapsis was seen between the longest and the smallest (faster) homologs, all observed wild-type nuclei showed a regular synchrony of pairing between bivalents (Figure 7a). At late zygotene, mostly only one or two of the bivalents (often among the three longest) remained unpaired for 5 to 15% of their lengths and failure to pair was clearly associated with interlockings, *i.e.*, the entrapment of bivalents or axial elements between the homologs of another partially paired bivalent.

Such a high degree of synchrony was not found in the mutants. In +/*76* nuclei (Figure 7b), the interbivalent differences ranged from 50 to 65% at mid-zygotene, and at late zygotene remained as high as 55% in some nuclei: 100% pairing for most bivalents but only 45–75% pairing in one or two of the homologs, independently of their length and not always connected to interlocks. This asynchrony was even higher in the *asy2-17/asy2-17* nuclei where completely unpaired homologs were present in all early and mid-zygotene nuclei (Figure 7c). At late zygotene the differences of pairing ranged from 10 to 100% irrespective of chromosome length, and telomeres were usually found to be the last regions to complete pairing. This unsynchronized pairing of the mutant strains cannot be attributed to a difference in interlocking rates, because these rates were similar in the three strains: around 40% in wild type, 45% in +/*76* and 40% in *asy2-17/asy2-17*.

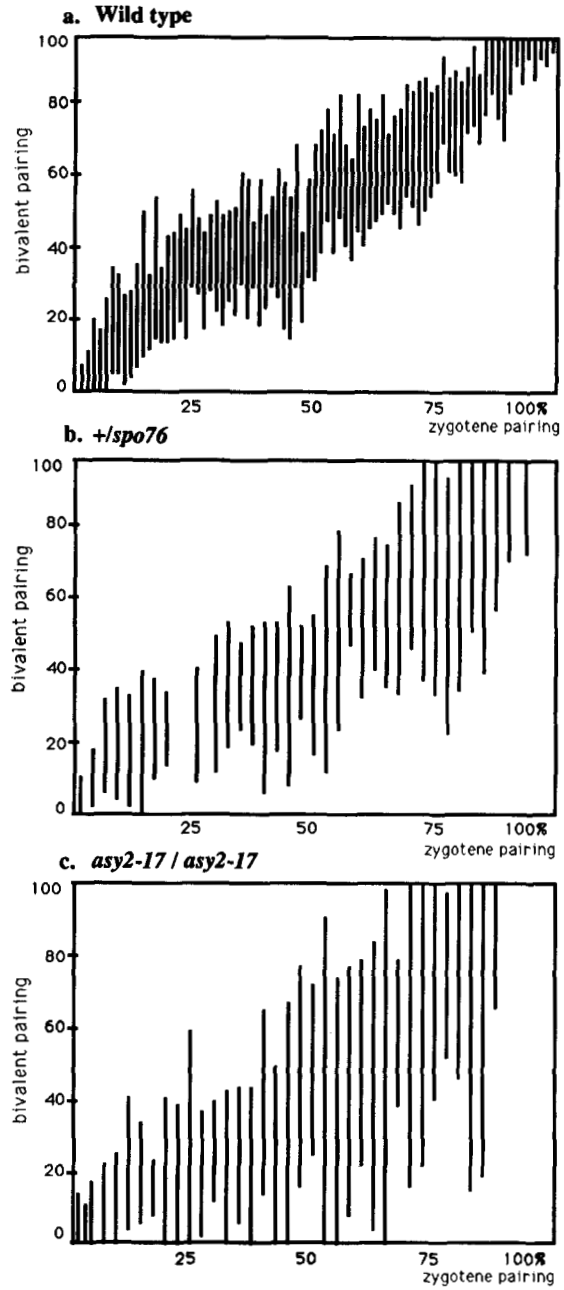

FIGURE 7.—Comparison of the extent of pairing within individual nuclei. Each axis represents percentage of pairing: abscissa indicates the extent of zygotene pairing and ordinate shows the maximum and minimum of bivalent pairing in the same nucleus (each vertical line represents one nucleus). **a**, In wild-type nuclei, there is a clear progression throughout zygotene. **b**, The lack of synchrony between the seven bivalents of +/*spo76*. This retardation of the pairing progress is even more accentuated in *asy2-17/asy2-17* (**c**).

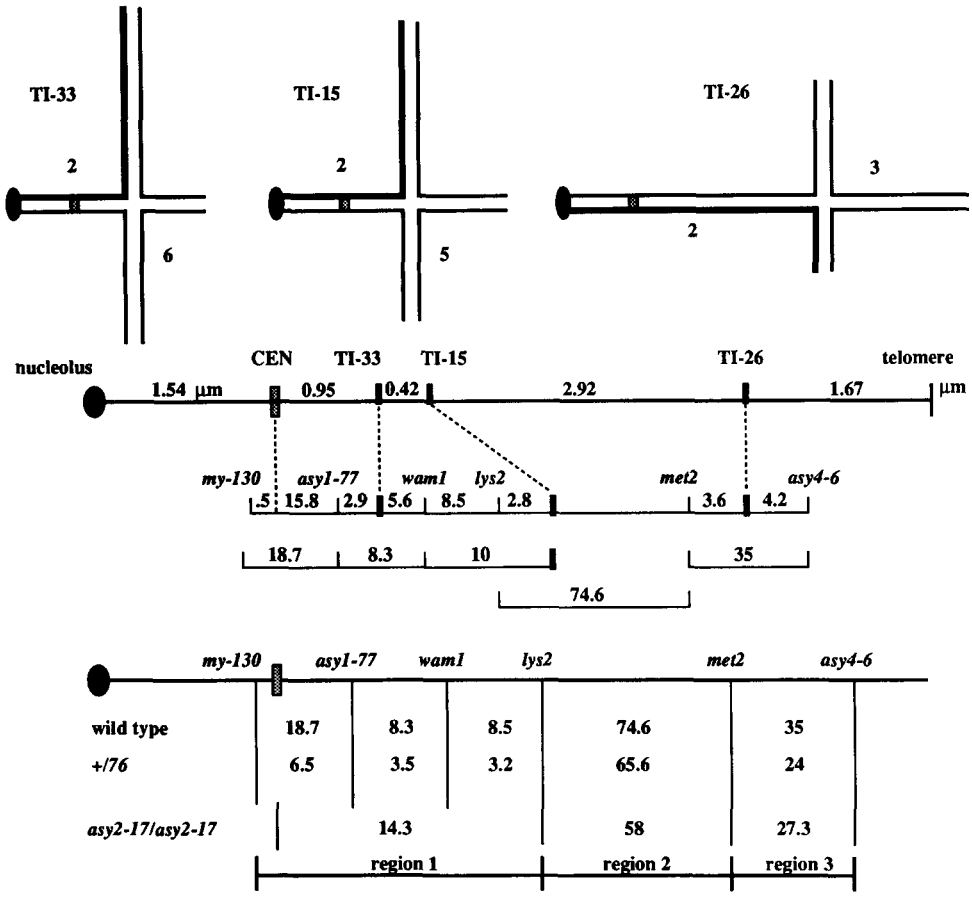

FIGURE 8.—Physical and genetic maps of chromosome *2*. Three heterozygous translocation crosses illustrate the physical mapping. Bold arms correspond to chromosome *2*. Number on the right corresponds to the second chromosome involved in the translocation. Genetic markers used and map distances are shown beneath the diagram of chromosome *2*. The lower part of the figure gives the comparison between wild-type and mutant map distances in three regions of chromosome *2*.

In both mutants, the unpaired axial elements persisting to the end of prophase showed occasional thickenings. In 50% of the *asy2-17/asy2-17* nuclei at least one axial element was broken compared to 2% in wild type and 21% in *+/76* nuclei.

The effect of the mutants on exchange frequencies in a defined chromosome arm: Nucleolus organizer chromosome *2* was used because it is clearly identifiable in all nuclei, the rDNA of *S. macrospora* forming a terminal segment on the small arm. Its mean length, estimated in 42 late zygotene and early pachytene nuclei, was 7.5 μm (range 7–8.4 μm, second longest chromosome) with a relative bivalent length of 16.36 (standard deviation: 0.14), the total SC length being 45.8 μm. The mean centromere index (length of the short arm × 100/total length of the bivalent) measured by centromere differentiation on the SC was 20.67 (SD: 0.20).

Five genes were mapped on the long arm of chromosome *2* (Figure 8). In *+/spo76* and *asy2-17/asy2-17*, map distances (from crosses with two and three linked markers) were found to be reduced (45% and 66% of control, respectively) in all studied intervals (Figure 8 and Table 3).

To correlate genetic maps with physical intervals, we analyzed the synaptic configurations of three reciprocal translocations: TI-33 (chromosomes *2* and *6*), TI-15 (*2*; *5*) and TI-26 (*2*; *3*) with a breakpoint in the long arm of chromosome *2*. Heterozygotes for each translocation were serially sectioned; all showed the typical cross shape at pachytene and the measurement of arm lengths using SC lateral elements is sufficiently precise to allow localization of breakpoints on a chromosome. Ten pachytene nuclei were reconstructed for each translocation and the breakpoints located on the SC (Figure 8). The long arm could thus be divided into four intervals: centromere–TI-33 = 0.95 μm, TI-33–TI-15 = 0.42 μm, TI-15–TI-26 = 2.92 μm and TI-26–telomere = 1.67 μm, corresponding to 16, 7, 49 and 28% of the SC length measured from centromere to telomere (Figure 8). In wild type, the known genetic markers of chromosome *2* were mapped relative to the translocation breakpoints and their map distances are given Figure 8 (see Table 3 for corresponding tetrads).

The genetic map-SC length bounds were estimated in three regions: region 1 = *my-130* (on the small arm, at 0.5 map unit from the centromere)–*lys2*, region 2 = *lys2–met2* and region 3 = *met2–asy4-6* (Figure 8). The length of *lys2*–TI-15 being unknown, the total length of region 1 was calculated in two ways. The 2.8 map distance *lys2*–TI-15 being 8% of the centromere–TI-15 distance, length of region 1 would be 1.37 μm (0.95 + 0.42) × 0.92 = 1.26 μm. The other

TABLE 3

Tetrad types and map distances of chromosome 2

Interval	Ascus types observed PD	T	NPD	Map length
Wild type				
my-130–centromere	93	1	0	0.5
Centromere–*asy1-77*	67	31	0	15.8
asy1-77–TI-33	32	2	0	2.9
TI-33–*wam1*	32	4	0	5.6
wam1–lys2	351	72	0	8.5
lys2–TI-15	33	2	0	2.8
lys2–met2	(a) 12	47	8	74.6
	(b) 11	72	14	
met2–TI-26	13	1	0	3.6
TI-26–*asy4-6*	22	2	0	4.2
my-130–asy1-77	115	69	0	18.7
asy1-77–wam1	160	32	0	8.3
wam1–TI-15	31	8	0	10
met2–asy4-6	45	67	2	35
+/76				
my-130–asy1-77	87	13	0	6.5
asy1-77–wam1	251	19	0	3.5
wam1–lys2	(c) 125	10	0	3.2
	(d) 132	4	0	
lys2–met2	(e) 8	11	5	65.6
	(f) 8	27	2	
met2–asy4-6	35	21	1	24
asy2-17/asy2-17				
Centromere–*lys2*	(g)			14.3
lys2–met2	23	45	7	58
met2–asy4-6	64	53	2	27.3

(a) If *my-130–lys2* = T (59% asci); (b) if *my-130–lys2* = PD or NPD (41% asci). (c) If *my-130–wam1* = T (23% asci); (d) if *my-130–wam1* = PD or NPD (77% asci). (e) If *my-130–lys2* = T (40% asci); (f) if *my-130–lys2* = PD or NPD (60% asci). (g) 46 SDS/161 total; SDS = second division segregation. PD = parental ditype; T = tetratype; NPD = nonparental ditype.

TABLE 4

Exchange frequencies in three regions of chromosome 2

my-130–lys2 region 1 Cen–*wam1–lys2*	*lys2–met2* region 2	*met2–asy4-6* region 3
Wild type		
E_0:39%	E_0:5%; E_1:51%; E_2:44%	E_0:31%; E_1:60%; E_2:9%
45 PD PD	7PD-33T-5 NPD	3-3-1; 9-24-0; 3-2-0
E_1:49%	E_0:5%; E_1:59%; E_2:36%	E_0:43%; E_1:50%; E_2:7%
16 PD T	3 PD-11 T-2 NPD	1-2-0; 3-7-1; 1-1-0
40 T PD	5 PD-32 T-3 NPD	2-3-0; 17-15-0; 1-2-0
E_2:12%	E_0:8%; E_1:92%; E_2:0%	E_0:38%; E_1:62%; E_2:0%
13 T T	1 PD-12 T-0 NPD	0-1-0; 5-7-0; 0-0-0
+/76		
E_0:54%	E_0:19%; E_1:70%; E_2:11%	E_0:77%; E_1:23%; E_2:0%
70 PD PD	15 PD-53 T-2 NPD	8-7-0; 44-9-0; 2-0-0
E_1:46%	E_0:10%; E_1:30%; E_2:60%	E_0:65%; E_1:35%; E_2:0%
4 PD T	0 PD-4 T-0 NPD	0-0-0; 2-2-0; 0-0-0
56 T PD	15 PD-32 T-9 NPD	7-8-0; 21-11-0; 9-0-0

E_0 = zero exchange; E_1 = one exchange; E_2 = two exchanges. PD = parental ditype; T = tetratype; NPD = nonparental ditype. In the tetrad data, region 1 is cut by *wam1* (see Figure 8) and the tetrad distribution is given for both intervals. In region 3 the tetrad types are always given in the same order: PD-T-NPD. For example 3-3-1 means that among the 7 PD found in region 2 the tetrad distribution in region 3 was 3 PD-3 T-1 NPD. Similarly, 9-24-0 and 3-2-0 are, in region 3, the tetrad distributions of respectively the 33 T and 5 NPD observed for region 2.

estimation was to say that the TI-33–*lys2* map distance represents 83% of the TI-33–TI-15 map distance. Assuming that the translocations display no crossover depression (which appears to be the case for TI-33, see map distances in Figure 8), the SC length TI-33–*lys2* is 0.42 μm (length TI-33–TI-15) × 0.83 = 0.35 μm. The total length of region 1 would thus be 0.95 + 0.35 = 1.3 μm. The number of exchanges in region 1 was also calculated from two sets of data: 0.65 when based on the small map distances: centromere - *asy1–77*, *asy1-77–wam1* and *wam1–lys2* (see tetrad distribution in Table 3) and 0.72 when based on the data obtained from the crosses used in Table 4. On the basis of a Poisson distribution, 1% of triple exchange would be expected for a mean of 0.65 exchange. Among the 423 tetrads analyzed (triple marker cross *my-130 wam1 lys2*), none showed a triple exchange. This gives a range from 0.50 (0.65 per 1.3 μm) to 0.57 (0.72 per 1.26 μm) exchange per μm of SC in region 1.

In region 3, Figure 8 shows clearly that TI-26 reduced exchange frequencies in the region surrounding the breakpoint: 35 map units between *met2* and *asy4-6* compared to their respective 3.6 and 4.2 map distances to TI-26. This effect on recombination is in good agreement with the electron microscopy observations, where TI-26 showed delayed pairing in the middle part of the quadrivalent until mid-pachytene, when TI-33 and TI-15 showed effective pairing in all reconstructed pachytene quadrivalents. Based on Table 4, 0.69 exchanges were observed in region 3. Exchange frequencies being similar to region 1 and double exchange events fewer than in region 1 (see Table 4), the probability of triple exchanges was hypothesized as zero. Length of region 3 was thus estimated to range from 1.21 μm to 1.38 μm (using either 0.72 exchange per 1.26 μm or 0.65 per 1.3 μm of region 1).

In region 2, 1.3 and 1.46 exchanges were calculated from respectively Table 3 and Table 4. Those estimations did not take into account triple exchange events. In the middle region *lys2–met2*, where no internal marker is known, for a mean of 1.4 exchanges, 11% of triple exchanges are predicted. The estimated exchange frequency for this region would thus range from 1.5 to 1.6. Assuming an equal depression on both sides of TI-26 (*met2*–TI-26 = 0.6 or 0.69 μm), region 2 lengths would range from 2.30 to 2.43 μm (2.92 − 0.69 + 0.07 to 2.92 − 0.6 + 0.11). This gives a range of 0.62 to 0.69 exchange per μm of SC. If *met2* is shifted close to TI-26, this number would

be 0.55 exchange per μm (1.6 exchange/2.92 μm).

With reasonable precision, the number of exchanges occurring between centromere and *asy4-6* in the wild-type strain ranged from 2.84 to 3 per meiosis. In +/*76*, 5% of the meioses showed zero exchange and the mean value of exchange in the centromere–*asy4-6* interval was reduced. It ranged from 1.93 (0.46, 1.19 and 0.28 based on Table 4) to 2.04 (0.26, 1.31 and 0.47 based on Table 3). The average number of exchange detected per meiosis in *asy2-17/asy2-17* was 1.9 exchange (0.28, 1.07 and 0.55 based on Table 3).

Correspondence of crossing overs to large nodules: Calculated from mid-zygotene to mid-pachytene (Figures 9, 10 and 11), the mean number of LN found in chromosome *2* was: 4.2 ± 0.7 in wild type (4.42 ± 0.6 from early pachytene nuclei), 2.76 ± 0.7 in +/*76* and 2.5 ± 0.7 in *asy2-17/asy2-17*. Although there was an equivalent LN and recombination decrease in the two mutants, almost 100% of the nuclei showed one LN (located at various positions between nucleolus and centromere) in the small arm of chromosome *2* (Figures 9, 10 and 11). Thus the LN deficiency is not evenly distributed across chromosome *2*.

The mean number of LN in the three regions of chromosome *2* investigated for recombination are shown in Table 5. This Table also shows the exchanges found in the same regions in the three strains (see above). In wild type, the LN numbers were closely equivalent to exchange frequencies in each of the three analyzed regions. Strain +/*76* exhibited a difference between the two values in the same three regions. The deficit of LN seen in region 2 could be due to the fact that *met2* and *asy4-6* were located at equivalent distances from the TI-26 breakpoint and that the correlation between map units and μm of SC was estimated from region 1. A closer equivalence between LN and exchange could be obtained in region 3 if the physical distances of *met2* and *asy4-6* to TI-26 were reduced, allowing a shift of part of the LN counted for region 3 to region 2. However, even if the distance *met2*–TI-26 was zero, the number of LN in region 2 would increase from 0.40 to 0.47, which remains far from the 1.19 or 1.31 exchanges measured in region 2. In *asy2-17/asy2-17* the comparison between the observed LN and exchanges found in the three regions showed that LN and exchange were equivalent in region 1 while a deficit of LN was observed in regions 2 and 3 (Table 5). A better equivalence in the third region could be obtained by shifting *asy4-6* toward the telomere, but the numbers do not correlate in region 2, whatever the location of *met2* might be.

Due to the lack of genetic markers, comparison of exchange and LN distribution cannot be made in the distal *asy4-6*–telomere region (1 μm of SC). Despite the depletion of exchange and LN observed in the mutants along the rest of this arm, the number of LN in this distal region was similar in the three strains

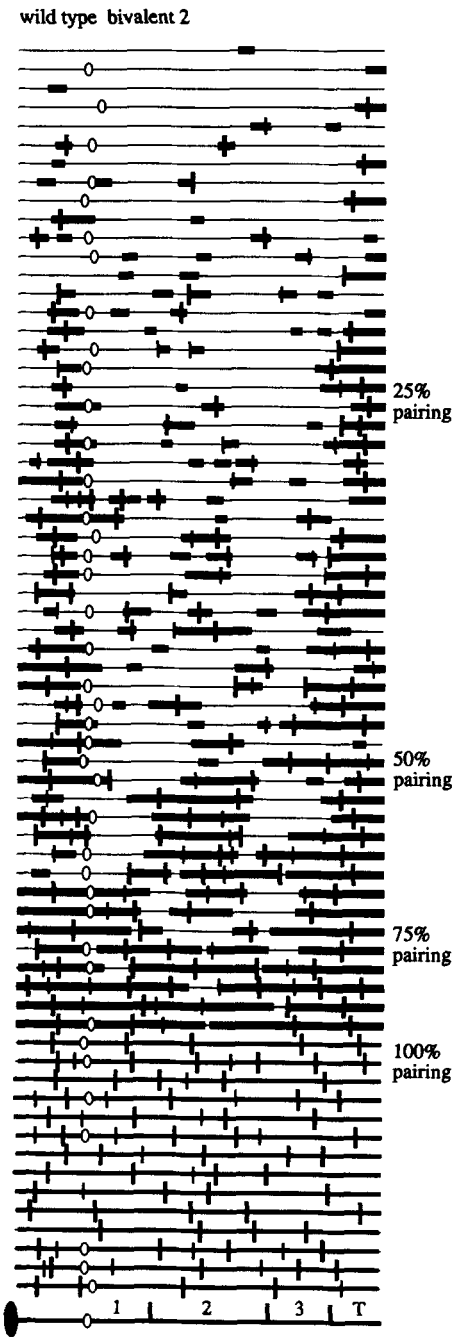

FIGURE 9.—Pairing pattern and nodule location of chromosome 2 (normalized by HP 1000) as mapped in 67 wild-type nuclei. These chromosomes were chosen as having centromere positioning so that nodules could be unambiguously placed in the centromere region, and no interlockings. Bold lines represent SC. Fine lines correspond to unpaired regions. In representation of 100% paired chromosomes, although SC was continuous, it is not shown in bold for easier legibility. Bold rectangles transecting SC denote large nodules and fine smaller transverse lines, small nodules. Unfilled ovals show the position of centromeres. At bottom is a representation of the normalized chromosome 2, indicating the nucleolus (filled oval), centromere (small unfilled oval), the three regions studied (1–3) and the telomeric region (T).

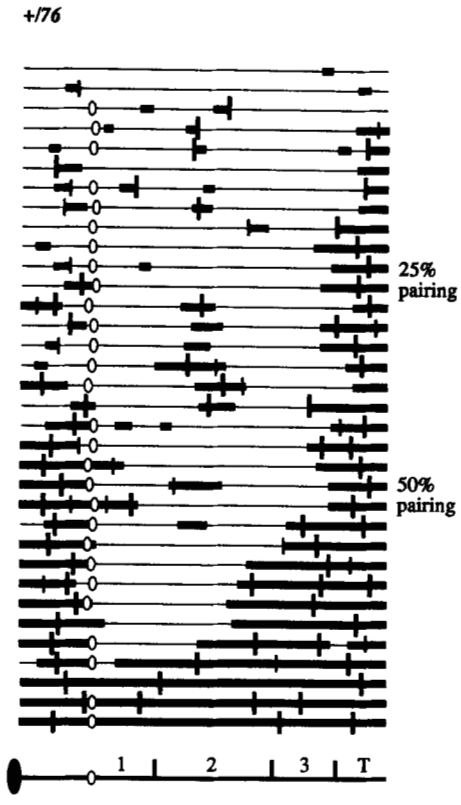

FIGURE 10.—Pairing pattern and nodule location of chromosome 2 in 34 nuclei of +/76, illustrating the depression of pairing in the mid-region of the long arm. Presentation is the same as that shown in Figure 9.

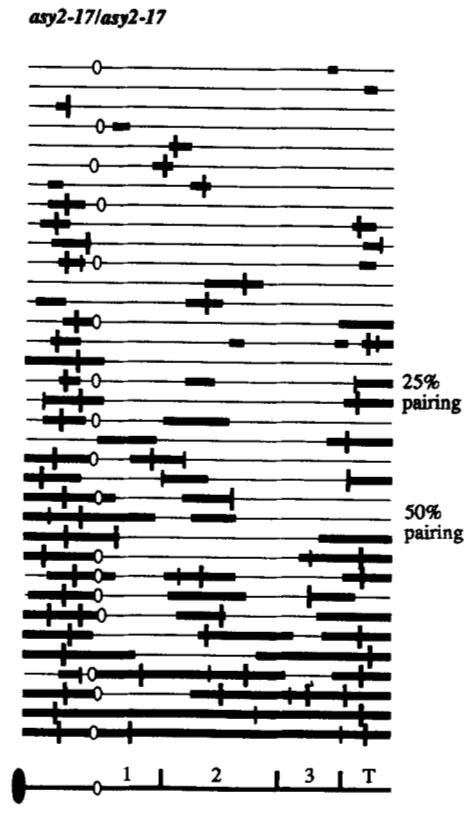

FIGURE 11.—Pairing pattern and nodule location of chromosome 2 in 35 nuclei of *asy2-17/asy2-17*, illustrating the delayed pairing in the telomeric regions and the wild-type pairing of the small arm despite a pairing depression in the long arm (compare with Figure 9). Presentation is the same as that shown in Figure 9.

(Table 5). In wild-type 0.62 LN in 1 μm of SC correlates with the 0.50–0.57 LN per μm found in region 1. On the other hand, in the mutant nuclei, a clear excess of LN was found in this terminal region compared to the 0.15 and 0.25 LN respectively found in region 1 (Table 5). Thus, the two mutants showed region-specific effects on LN location.

LN distribution can be related to the pairing pattern along chromosome 2 (compare Figure 10 and 11 with Figure 9). In +/76, pairing was mostly initiated in the short arm and at the telomeres. Most late zygotene nuclei had a deficit of pairing in regions 1 and 2, and progression in pairing appeared mainly as an elongation of the telomeric initiation with a clear rupture of elongation at the centromere (Figure 10). This pairing pattern correlated with the 78% and 71% reduction of LN observed in regions 1 and 2 and with the fact that in region 3 as well as in the telomeric region, LN numbers were close to wild type.

Chromosome interference was compared between wild type and mutants. In region 1 (crosses with three linked markers), when no exchange occurred between *my-130* and *asy1-77*, *asy1-77* lay 23 map units (72 PD:41 T:2 NPD) from *lys2*; with one exchange, this distance was only 15 units (48:21:0). The same reduction was observed when region 1 was cut by *wam1*: no exchange between *my-130* and *wam1* gave a distance of 11 units (150:42:0) between *wam1* and *lys2* and 6 units (148:23:0) when one exchange had occurred. Such results indicated clearly that the presence of one exchange in the first part of this region reduced the probability of a second exchange in the adjacent area. Coefficients of coincidence in region 1, cut by *wam1* was 0.75 (number of double exchanges expected: $0.178 \times 0.48 = 0.0856$; number observed: $0.135 \times 0.48 = 0.0646$) and 0.75 when cut by *asy1-77* (number of double exchanges expected: $0.40 \times 0.375 = 0.15$; observed: $0.30 \times 0.375 = 0.112$), confirming positive interference between crossovers in region 1.

In the crosses with five linked markers used for Table 4 (including *my-130*, *wam1*, *lys2*, *met2* and *asy4-6*), 130 tetrads were analyzed but all markers were legible only in 114 tetrads. In the 121 tetrads (17 PD:92 T:12 NPD) analyzable for region 2, tetratypes are significantly greater than 2/3 (P from $\chi^2 < 0.05$) indicating a positive interference between exchanges. In the third region, where observed numbers were 45:67:2, the PAPAZIAN (1952) formula (NPD = $1/8\ T^2(1 + 3/2\ T)$) gives a no-interference expectation of 37:67:10.

In region 1 of +/76, when no exchange occurred between *my-130* and *asy1-77*, *asy1-77* lay 8.1 map units (103:20:0) from *lys2*; with one exchange, this distance

TABLE 5

Comparison of exchanges and LN

		Region				
		1	2	3	Total 1-3	*asy4-6*–telomere
Wild type	Exchange	0.65–0.72	1.5–1.6	0.69	2.84–3	NT
	LN	0.58	1.38	0.69	2.65 ± 0.8	0.62
+/76	Exchange	0.26–0.46	1.19–1.31	0.28–0.47	1.93–2.04	NT
	LN	0.15	0.38	0.61	1.15 ± 0.8	0.61
asy2-17/asy2-17	Exchange	0.28	1.07	0.55	1.9	NT
	LN	0.25	0.38	0.16	0.83 ± 0.7	0.66

NT = not tested.

was 2.8 units (51:3:0). The same reduction was observed when region 1 was cut by *wam1*: no exchange between *my-130* and *wam1* gave a distance of 3.7 units (125:10:0) between *wam1* and *lys2* and 1.5 units (132:4:0) when one exchange had occurred. Such results indicated that the presence of one exchange in the first part of this region reduced the probability of a second exchange in the adjacent area. Strain *+/76* exhibited negative interference between regions 1 and 2: although there was a general decrease of exchanges, in the 54% of meioses with no exchange in region 1 (Table 4), region 2 had 0.93 exchange, whereas among the 46% with one exchange in region 1, region 2 had 1.5 exchanges, which is significantly higher. Contrary to the wild-type situation, in *+/76*, when one exchange occurred in region 1, an excess of two exchanges (60% compared to 36% in wild type) was found in region 2 (Table 4).

When one exchange was seen in region 1 in *asy2-17/asy2-17*, region 2 exhibited an exchange distribution (2:18:4) similar to the wild-type situation (8:43:5). When zero exchange occurred in region 1, a 50% decrease (21:27:3) of the exchange frequencies was found in region 2 indicating, like in *+/76*, a negative interference between region 1 and 2. The same negative interference was also observed for region 3:0.33 exchange (26:13:0) when *met2* segregated during first division and 0.58 exchange (38:40:2) when *met2* segregated during second division.

DISCUSSION

The decrease of crossover events in the two mutants of *S. macrospora* is accompanied by, or results in, modifications of the pattern of pairing initiation. Moreover, the decrease of meiotic exchanges (crossing over and conversion) parallels the decrease of both types of nodules: the recombination nodules believed to mark the sites of crossovers (reviewed in CARPENTER 1988), called here large nodules, and the small nodules hypothesized to be related to conversion (RASMUSSEN and HOLM 1978; CARPENTER 1979b). Despite the twofold exchange decrease, sections of the genome such as the short arm of chromosome 2 and telomere regions are sheltered from nodule decrease and from pairing modifications.

Inconsistencies concerning the relationship between pairing and recombination stem from the lack of comparable SC and recombination data. What do we learn from our study? First, the general decrease of crossover events in two mutants correlates with a general decrease of the number of SC segments. This correlation is not only quantitative, since exchange distribution parallels SC-site localization in the long arm of chromosome 2. Second, pairing modifications are not evenly distributed along the bivalents, implying several steps of control. The relationship between pairing pattern and chiasmata was examined in two Allium species which show complete pairing but clear differences in the localization of their chiasmata. Although initiation and progression of pairing in the two species were slightly different, the pairing pattern was essentially the same, suggesting that the sequence of pairing does not influence chiasma localization (ALBINI and JONES 1987, 1988). This result is not in contradiction with our observations indicating that pairing pattern may be involved in the regulation of frequency and distribution of exchanges. The number of initiation sites seen in Allium is substantially higher than the number of chiasmata and SC nodules. Thus, only some of the observed initiation sites may be necessary for recombination events, either because they will establish areas where exchange can happen, or because they are initiated at the right time for promoting crossovers. The supernumerary pairing sites could be used for synapsis progression, which fits well with the observation that higher plants with long SC show the highest number of initiation sites (LOIDL 1990).

Besides the mutant effects, a second example of a possible correlation between pairing and recombination is given by the heterozygous TI-26 translocation of Sordaria, where delayed SC formation on both sides of the breakpoint parallels a deficit in crossover events over a minimum distance of 35 map units (as

seen above). Causality between synapsis and chiasma frequencies was also suggested by the results of chromosome rearrangements in several other species (MAGUIRE 1977, 1986; PARKER 1987; CAWOOD and BRECKON 1989; GORLOV *et al.* 1991). Another example of an interrelation between chiasma formation and pairing behavior is suggested by the very intriguing effect of B chromosomes on chiasma frequency in the A-set, seen in many organisms. Individual modifications of chiasma position in A-chromosomes, together with a remarkable increase of their SC lengths (50% with two Bs) were observed in *Crepis capillaris* (JONES, WHITEHORN and ALBINI 1989; PARKER *et al.* 1990). Individual response of chromosomes as well as increase in chiasma number when SC lengthen could be explained by the model of JONES (1974), suggesting that bivalents contain a large number of potential chiasma sites, each site having a uniform but low probability of chiasma formation. When the conditions change as in SC lengthening or structural chromosome change, sites not used normally will become active.

A second question which deserves consideration is that of the relation of gene conversion to synapsis (SMITHIES and POWERS 1986; CARPENTER 1987). Conversion via strand exchange (CARPENTER 1987) or direct DNA-DNA interactions, through the interspersed late replicating sequences (zyg DNA) found in Lilium (STERN and HOTTA 1977), were proposed as possible mechanisms for identifying homology. Occurrence of site-specific double-strand breaks in the vicinity of recombination hot spots and their accumulation in the yeast *rad50S* mutant in the absence of SC formation suggest another probable mechanism through which the recombination machinery could be involved in homology search and SC formation (ALANI, PADMORE and KLECKNER 1990; CAO, ALANI and KLECKNER 1990). CARPENTER (1987) proposed that the early nodules hypothesized to be related to gene conversion (called here small nodules because their temporal appearance was less evident in Sordaria than in Drosophila), mediate this homology search. The strongest support for a correlation between conversion and SC pairing is given by the phenotype of the yeast *mer1* mutant, displaying reduced levels of recombination and poor SC assembly, in which the conversion and SC defects can be corrected by *mer2* without correcting the crossover defect (ENGEBRECHT, HIRSCH and ROEDER 1990). The observation presented here, that a parallel decrease of small nodules and conversion rate (with the restriction that only one gene was studied) correlates with pairing deficit in the two Sordaria mutants, is consistent with the hypothesis of a possible involvement of conversion and/or small nodules in homologous recognition and SC initiation.

What can we learn from this study about the role, if any, of the large nodules in recombination? In wild-type *S. macrospora* small (SN) and large (LN) nodules appear at zygotene. Only LN remain after mid-pachytene and their number, observed in the SC segments maintained at diplotene, correspond to the number of chiasmata (here, and ZICKLER 1977). This parallels the observation of morphological continuity between nodules and chiasmata found in some organisms (VON WETTSTEIN, RASMUSSEN and HOLM 1984). The distribution and number of LN along chromosome 2 in wild-type Sordaria correlates precisely with the exchange distribution determined genetically. The positioning of LN, recorded along all bivalents, showed interference with one another, as expected if they correspond to crossing over. Moreover, here, as well as in Drosophila (CARPENTER 1979a), LN frequency responds to events that perturb the number of crossovers. These observations lend strong support for a role of these structures in meiotic exchanges (reviewed in CARPENTER 1988). However, the question of their location at sites where crossing over has occurred remains open. Drosophila *mei-9* mutant showed wild-type numbers and locations of nodules although drastic crossing over reduction, leading to the suggestion that LN mark the sites of precondition functions of crossing over (CARPENTER 1979a). Here, although there was good general correlation between LN and exchange frequencies, neither in *+/76* nor in *asy2-17/asy2-17*, did LN numbers coincide with the exchange frequency in all three studied regions of chromosome 2. The number of LN seen in the mutant meioses may be underestimated for at least three reasons. In *asy2-17/asy2-17*, 5% of asci show aneuploidy and those tetrads would not be included in the exchange data, which would thus show a slight excess of exchange compared to LNs. This is not true for *+/76* which shows wild-type sporulation. Another argument would be that the mutant defects could be a shorter lifetime of the LN. And finally, although the wild-type data indicate that LN are stable from pachytene to diplotene, in the mutants, LN could have departed from the SC before pachytene because of the delayed pairing even if LN have the normal life span.

Coincidence of LN and exchange may arise because both are influenced by the initiation, the sequence or the extent of SC formation. First, distribution of LN, recorded along the bivalents, is not random: low around the centromeres, medium in the middle of all long arms and high in the distal regions (data not shown). In order to account for crossing over and chiasma interference, several proposals have been made invoking limiting supply of a substance or proposing that the first successful crossover event causes a signal transmitted along the SC, inhibiting the installation of additional nodules and releasing nodules

which are not yet involved in recombination process (HOLLIDAY 1977; EGEL 1978; HOLM and RASMUSSEN 1983; JONES 1984, 1987; STACK and ANDERSON 1986b; MAGUIRE 1988; BOJKO 1989; KING and MORTIMER 1990). It is worth noting that, in Sordaria, the modified interference pattern shown by the mutants can be related to differences in initiation and extension of the SC at zygotene. On the other hand, the pairing initiation sites observed during zygotene did not all contain nodules. The percentage of SC segments with nodules was found to be similar in wild-type and mutant zygotene nuclei although there was a general decrease of the number of sites in both mutants, suggesting that the primary defect of the mutants was pairing. Fewer sites will give rise, by pairing elongation, to more SC regions devoid of nodules. Finally, it has been shown clearly that LN localization arises mostly from the tendency of nodules to occur preferentially in certain regions, like the small arm of chromosome 2, or all telomere regions (data not shown). Similar nonrandom distribution was observed in several species (VON WETTSTEIN, RASMUSSEN and HOLM 1984; BOJKO 1989). Here these regions are also the regions where pairing initiates first. According to these observations, interference and nodule localization is suggested to be the indirect expression of pairing pattern, at least in *S. macrospora*. Moreover, the two mutants showed that in the areas where preferential pairing initiation was found, LN were unaffected (the short arm) or more slightly affected (the telomeric region). The same difference was also obvious in the other bivalents (data not shown). Such diversity in the recombination control was previously described at several levels. Occurrence of independent control of recombination at specific sites was found in *Neurospora crassa* (CATCHESIDE 1986). Variation in the control of recombination in specific localized regions was established in yeast by comparing strains obtained from different sources (SIMCHEN and STAMBERG 1969). Finally, control at the level of the chromosome was discovered by PARKER (1975). These observations imply that a mechanism which functions in the production of genetic exchange is, at the same time, acting to restrict exchange levels in some parts of chromosomes more than others. The coordinate response of pairing constraints on crossing over and nodule distribution in both mutants suggests that these two phenomena may be causally related.

Two categories of recombination mutants had been recognized by SANDLER *et al.* (1968): those that affect crossing over distribution by altering preconditions for exchange, and those that affect the probability of exchange without affecting the preconditions and so do not influence exchange distribution. The mutants studied here belong to the first category.

Special thanks are due to ANGELOS KALOGEROPOULOS for writing the HP 1000 computer program used in this study. We would like to gratefully acknowledge DAVID D. PERKINS for helpful comments and ADELAIDE T. C. CARPENTER for critical reading of the manuscript and many valuable suggestions. Finally, we are grateful to ALMUTH COLLARD for her patience and friendship in serial sectioning and printing all nuclei. This research was financially supported by the Centre National de la Recherche Scientifique (URA 1354).

LITERATURE CITED

ABIRACHED-DARMENCY, M., D. ZICKLER and Y. CAUDERON, 1983 Synaptonemal complex and recombination nodules in rye (*Secale cereale*). Chromosoma **88:** 299–306.

ALBINI, S. M., and G. H. JONES, 1987 Synaptonemal complex spreading in *Allium cepa* and *A. fistulosum*. I. The initiation and sequence of pairing. Chromosoma **95:** 324–338.

ALBINI, S. M., and G. H. JONES, 1988 Synaptonemal complex spreading in *Allium cepa* and *Allium fistulosum*. II. Pachytene observations: the SC karyotype and the correspondence of late recombination nodules and chiasmata. Genome **30:** 399–410.

ALANI, E., R. PADMORE and N. KLECKNER, 1990 Analysis of wild type and *rad50* mutants of yeast suggests an intimate relationship between meiotic chromosome synapsis and recombination. Cell **61:** 419–436.

BAKER, B. S., A. T. C. CARPENTER, M. S. ESPOSITO, R. E. ESPOSITO and L. SANDLER, 1976 The genetic control of meiosis. Annu. Rev. Genet. **10:** 53–134.

BHARGAVA, J., J. A. ENGEBRECHT and G. S. ROEDER, 1992 The *rec102* mutant of yeast is defective in meiotic recombination and chromosome synapsis. Genetics **130:** 59–69.

BERNELOT-MOENS, C., and P. B. MOENS, 1986 Recombination nodules and chiasma localization in two Orthoptera. Chromosoma **93:** 220–226.

BOJKO, M., 1989 Two kinds of "recombination nodules" in *Neurospora crassa*. Genome **32:** 309–317.

CAO, L., E. ALANI and N. KLECKNER, 1990 A pathway for generation and processing of double-strand breaks during meiotic recombination in *S. cerevisiae*. Cell **61:** 1089–1101.

CARPENTER, A. T. C., 1979a Recombination nodules and synaptonemal complex in recombination-defective females of *Drosophila melanogaster*. Chromosoma **75:** 259–292.

CARPENTER, A. T. C., 1979b Synaptonemal complex and recombination nodules in wild-type *Drosophila melanogaster* females. Genetics **92:** 511–541.

CARPENTER, A. T. C., 1987 Gene conversion, recombination nodules, and the initiation of meiotic synapsis. BioEssays **6:** 232–236.

CARPENTER, A. T. C., 1988 Thoughts on recombination nodules, meiotic recombination, and chiasmata, pp. 529–548 in *Genetic Recombination*, edited by R. KUCHERLAPATI and G. R. SMITH. American Society for Microbiology, Washington D.C.

CATCHESIDE, D. E. A., 1986 A restriction and modification model for the initiation and control of recombination in Neurospora. Genet. Res. **47:** 157–165.

CAWOOD, A. H., and G. BRECKON, 1989 Transmission of three radiation-induced translocations in the syrian hamster. I Chromosome studies of male meiosis: pachytene to metaphase II. Chromosoma **98:** 301–306.

CROFT, J. A., and G. H. JONES, 1989 Meiosis in *Mesostoma ehrenbergii*. IV. Recombination nodules in spermatocytes and a test of the correspondence of late recombination nodules and chiasmata. Genetics **121:** 255–262.

EGEL, R., 1978 Synaptonemal complex and crossing-over: structural support or interference? Heredity **41:** 233–237.

ENGEBRECHT, J., J. HIRSCH and G. S. ROEDER, 1990 Meiotic gene conversion and crossing over: their relationship to each other and to chromosome synapsis and segregation. Cell **62:** 927–937.

FLETCHER, H. L., 1977 Localized chiasmata due to partial pairing: a 3-D reconstruction of synaptonemal complexes in male *Stethophyma grossum*. Chromosoma **65:** 247–270.

GILLIES, C. B., 1985 An electron microscopic study of synaptonemal complex formation at zygotene in rye. Chromosoma **92:** 165–175.

GIROUX, C. N., 1988 Chromosome synapsis and meiotic recombination, pp. 465–496 in *Genetic Recombination*, edited by R. KUCHERLAPATI and G. R. SMITH. American Society for Microbiology, Washington D.C.

GORLOV, I. P., T. Y. LADYGINA, O. L. SEROV and P. M. BORODIN, 1991 Positional control of chiasma distribution in the house mouse. Chiasma distribution in mice homozygous and heterozygous for an inversion in chromosome 1. Heredity **66:** 453–458.

HASENKAMPF, C. A., 1984 Synaptonemal complex formation in pollen mother cells of *Tradescantia*. Chromosoma **90:** 275–284.

HENDERSON, S. A, 1988 Four effects of elevated temperature on chiasma formation in the locust *Schistocerca gregaria*. Heredity **60:** 387–401.

HOLLIDAY, R., 1977 Recombination and meiosis. Philos. Trans. R. Soc. Lond. Ser. B **227:** 359–370.

HOLM, P. B., 1977 Three dimensional reconstruction of chromosome pairing during the zygotene stage of meiosis in *Lilium longiflorum* (Thumb.). Carlsberg Res. Commun. **42:** 249–281.

HOLM, P. B., and S. W. RASMUSSEN, 1983 Human meiosis. VI. Crossing-over in human spermatocyte. Carlsberg Res. Commun. **48:** 385–413.

HUYNH, A. D., G. LEBLON and D. ZICKLER, 1986 Indirect intergenic suppression of a radiosensitive mutant of *Sordaria macrospora* defective in sister-chromatid cohesiveness. Curr. Genet. **10:** 545–555.

JONES, G. H., 1974 Correlated components of chiasma variation and the control of chiasma distribution in rye. Heredity **32:** 375–387.

JONES, G. H., 1984 The control of chiasma distribution, pp. 293–320 in *Controlling Events in Meiosis*, edited by C. W. EVANS and H. G. DICKINSON. The Company of Biologists Ltd., Cambridge.

JONES, G. H., 1987 Chiasmata, pp. 213–214 in *Meiosis*, edited by P. B. MOENS. Academic Press, London.

JONES, G. H., J. A. F. WHITEHORN and S. M. ALBINI, 1989 Ultrastructure of meiotic pairing in B chromosomes of *Crepis capillaris*. I. One-B and two-B pollen mother cells. Genome **32:** 611–621.

KING, J. S., and R. K. MORTIMER, 1990 A polymerization model of chiasma interference and corresponding computer simulation. Genetics **126:** 1127–1138.

LEBLON, G., D. ZICKLER and S. LE BILCOT, 1986 Most UV-induced reciprocal translocations in *Sordaria macrospora* occur in or near the centromere regions. Genetics **112:** 183–204.

LOIDL, J., 1987 Synaptonemal complex spreading in *Allium ursinum*: pericentric asynapsis and axial thickenings. J. Cell Sci. **87:** 439–448.

LOIDL, J., 1989 Effects of elevated temperature on meiotic chromosome synapsis in *Allium ursinum*. Chromosoma **97:** 449–458.

LOIDL, J., 1990 The initiation of meiotic chromosome pairing: the cytological view. Genome **33:** 759–778.

MAGUIRE, M. P., 1977 Homologous chromosome pairing. Philos. Trans. R. Soc. Lond. Ser. B **227:** 245–258.

MAGUIRE, M. P., 1986 The pattern of pairing that is effective for crossing-over in complex B-A chromosome rearrangements in maize. III. Possible evidence for pairing centers. Chromosoma **94:** 71–85.

MAGUIRE, M. P., 1988 Crossover site determination and interference. J. Theor. Biol. **134:** 565–570.

MOENS, P. B., and S. SHORT, 1983 Synaptonemal complexes of bivalents with localized chiasmata in *Chloealtis conspersa* (Orthoptera), pp. 99–106 in *Kew Chromosome Conference II*, edited by P. E. BRANDHAM and M. D. BENNETT. Her Majesty's Stationery Office, London.

MOREAU, P. J. F., D. ZICKLER and G. LEBLON, 1985 One class of mutants with disturbed centromere cleavage and chromosome pairing in *Sordaria macrospora*. Mol. Gen. Genet. **198:** 189–197.

OAKLEY, H. A., and G. H. JONES, 1982 Meiosis in *Mesostoma ehrenbergii* (Turbellaria, Rhabdocoela). I. Chromosome pairing, synaptonemal complexes and chiasma localisation in spermatogenesis. Chromosoma **85:** 311–322.

PADMORE, R., L. CAO and N. KLECKNER, 1991 Temporal comparison of recombination and synaptonemal complex formation during meiosis in *S. cerevisiae*. Cell **66:** 1239–1256.

PAPAZIAN, H. P., 1952 The analysis of tetrad data. Genetics **37:** 175–188.

PARKER, J. S., 1975 Chromosome specific desynapsis in *Hypochaeris radicata*. Chromosoma **49:** 391–406.

PARKER, J. S., 1987 Increased chiasma frequency as a result of chromosome rearrangement. Heredity **58:** 87–94.

PARKER, J. S., G. H. JONES, L. A. EDGAR and C. WHITEHOUSE, 1990 The population cytogenetics of Crepis capillaris. III. B-chromosome effects on meiosis. Heredity **64:** 377–385.

PERKINS, D. D., 1962 Crossing-over and interference in a multiply marked chromosome arm of Neurospora. Genetics **47:** 1253–1274.

RASMUSSEN, S. W., 1986 Initiation of synapsis and interlocking of chromosomes during zygotene in Bombyx spermatocytes. Carlsberg Res. Commun. **51:** 401–432.

RASMUSSEN, S. W., and P. B. HOLM, 1978 Human meiosis. II. Chromosome pairing and recombination nodules in human spermatocytes. Carlsberg Res. Commun. **43:** 275–327.

ROEDER, G. S., 1990 Chromosome synapsis and genetic recombination. Trends Genet. **6:** 385–389.

SANDLER, L., D. L. LINDSLEY, B. NICOLLETTI and G. TRIPPA, 1968 Mutants affecting meiosis in natural populations of *Drosophila melanogaster*. Genetics **60:** 525–558.

SIMCHEN, G., and J. STAMBERG, 1969 Fine and coarse controls of genetic recombination. Nature **222:** 329–332.

SMITHIES, O., and P. A. POWERS, 1986 Gene conversion and their relation to homologous chromosome pairing. Philos. Trans. R. Soc. Lond. Ser. B **312:** 291–302.

SOLARI, A. J., N. S. FECHHEIMER and J. J. BITGOOD, 1988 Pairing of ZW gonosomes and the localized recombination nodule in two Z-autosome translocations in *Gallus domesticus*. Cytogenet. Cell Genet. **48:** 130–136.

SPYROPOULOS, B., D. WISE and P. B. MOENS, 1989 Localized recombination nodules and sex chromosome behavior in the male mole cricket, *Neocurtilla hexadactyla*. Genome **32:** 275–281.

STACK, S. M., and L. K. ANDERSON, 1986a Two-dimensional spreads of synaptonemal complexes from solanaceous plants. II. Synapsis in *Lycopersicon esculentum* (tomato). Am. J. Bot. **73:** 264–281.

STACK, S. M., and L. K. ANDERSON, 1986b Two-dimensional spreads of synaptonemal complexes from solanaceous plants. III. Recombination nodules and crossing over in *Lycopersicon esculentum* (tomato). Chromosoma **94:** 253–258.

STACK, S. M., and D. L. SOULLIERE, 1984 The relation between synapsis and chiasma formation in *Rhoeo spathacea*. Chromosoma **90:** 72–83.

STERN, H., and Y. HOTTA, 1977 Biochemistry of meiosis. Philos. Trans. R. Soc. Lond. Ser. B **227:** 277–294.

SUDMAN, P. D., and I. F. GREENBAUM, 1990 Unequal crossing over and heterochromatin exchange in the X-Y bivalents of the deer mouse, *Peromyscus beatae*. Chromosoma **99:** 183–189.

THOMSON, R. L., M. WESTERMAN and N. D. MURRAY, 1984 *B* chromosomes in *Rattus fuscipes*. I. Mitotic and meiotic chromosomes and the effects of *B* chromosomes on chiasma frequency. Heredity **52:** 355–362.

VON WETTSTEIN, D., S. W. RASMUSSEN and P. B. HOLM, 1984 The synaptonemal complex in genetic segregation. Annu. Rev. Genet. **18:** 331–413.

ZICKLER, D., 1977 Development of the synaptonemal complex and the "recombination nodules" during meiotic prophase in the seven bivalents of the fungus *Sordaria macrospora* Auersw. Chromosoma **61:** 289–316.

ZICKLER, D., G. LEBLON, V. HAEDENS, A. COLLARD and P. THURIAUX, 1984 Linkage group-chromosome correlations in *Sordaria macrospora*: chromosome identification by three dimensional reconstruction of their synaptonemal complex. Curr. Genet. **8:** 57–67.

Communicating editor: P. J. PUKKILA